

Article

Late Tertiary Petrified Wood from Nevada, USA: Evidence of Multiple Silicification Pathways

George E. Mustoe

Geology Department, Western Washington University, Bellingham, WA 98225, USA;
E-Mail: mustoeg@wwu.edu; Tel: +1-360-650-3582

Academic Editor: James Schmitt

Received: 16 August 2015 / Accepted: 9 October 2015 / Published: 14 October 2015

Abstract: Late Tertiary fossil woods from the state of Nevada provide an opportunity for observing the mineralization sequences that cause buried wood to become permineralized. Oligocene and Miocene caldera basins contain abundant petrified wood that ranges in composition from incipient silicification to complete permineralization. Examination of specimens from 21 localities reveals that the petrifaction sequence can follow multiple pathways. Fossil wood specimens from a single stratum may have different mineralization; silicification may vary even within a single specimen. Despite these variations, several trends are evident. Features in Nevada specimens suggest that two fundamental processes are involved: early mineralization of cell walls, and later silica deposition in lumina, vessels, and rot pockets from groundwater that permeated these open spaces. The process of open-space filling may be analogous to the genesis of geodes and veins, where multiple episodes of hydrothermal precipitation may produce opal, chalcedony, and quartz as deposits within a single cavity. Silica polymorphs may coexist as primary precipitates, or they may originate from solid-state transformation of a single parent material. Relic lepisphere textures observed in some chalcedony wood specimens are evidence of opal→chalcedony transition. In Nevada, specimens that contain crystalline quartz, this mineral appears to have been formed by direct precipitation in open spaces, not from recrystallization of chalcedony. Opal-A has seldom been reported in fossil wood, but this amorphous material is fairly common in Nevada specimens.

Keywords: petrified wood; silica; opal; chalcedony; quartz; paleobotany; Nevada

1. Introduction

Previous interpretations of wood petrifaction have involved several approaches. One strategy utilizes observations of silicification of wood in modern hot-springs [1–4]. Mineralization occurs rapidly in these geothermal environments, but extremely high dissolved silica concentrations, elevated temperatures, and strongly oxidizing conditions provide a dissimilar match for depositional environments that produce most fossil wood. A second research strategy involves experimental studies where modern wood is exposed to silica-bearing solutions [5]. The practical need to produce silicification in a brief time period commonly involves use of synthetic silica compounds not found in nature (e.g., silanes or organosilicates), and elevated reaction temperatures.

A third strategy is based on petrographic observations of petrified wood, often from well-known fossil forests. Examples include Czech Republic (Late Pennsylvanian) [6], Chemnitz, Germany (Late Permian) [5,7,8], and Petrified Forest, Arizona, USA (Triassic) [9]. The study of very old petrified wood to infer initial phases of petrifaction poses significant analytical challenges. For example, Paleozoic and Mesozoic silicified woods almost invariably contain cryptocrystalline or microcrystalline quartz as the principal components, in contrast to opal that comprises many Cenozoic woods. This chronologic trend suggests that the composition of many Mesozoic woods have been transformed from their original mineralogy. Cathodoluminescence microscopy has been used in attempts to better understand the mineralogy of Mesozoic specimens [6,7,10,11], but determination of the original mineralization remains subjective.

This report describes silification processes based on analyses of Late Tertiary wood from 21 locations in Nevada, USA. These specimens record mineralization of plant tissue beginning at incipient stages and continuing thorough subsequent phases that resulted in complete permineralization.

2. Geologic Setting

The widespread abundance of silicified wood in the state of Nevada is related to the availability of silica as a result of episodes of rhyolitic volcanism. A fundamental tectonic process responsible for these volcanic events was the subduction of the Farallon Plate beneath the North America continental margin. Episodic eruptions produced large volumes of rhyolitic tephra that engulfed forests; caldera collapse produced topographic basins that allowed extensive accumulation of volcaniclastic sediments that preserved wood transported into ancient lakes by streams and mudflows. Twenty-three calderas have been identified in the Western Nevada Volcanic Field, and 14 additional rhyolitic ash-flow tuffs that presumably represent as-yet undiscovered calderas [12]. Radiometric ages indicate eruption and collapse of Western Nevada calderas occurred between 34.4 and 23.3 Ma. Calderas in the Southwestern Nevada Volcanic Field have ages ranging from >15 Ma to 7.5 Ma. [13]. Ash-flow tuffs in Western Nevada that were deposited during a 2 million year interval between 25.5 and 23.5 Ma [14]. These Oligocene-Miocene caldera deposits contain many fossil wood localities. In some locations, preservation of fossil wood continued into the early Pliocene, as lake basins created by caldera collapse continued to accumulate volcaniclastic sediment eroded from the adjacent uplands.

In northern Nevada, caldera development was triggered by the movement of the North America Plate over the Yellowstone Hot Spot, a body of magma situated in the upper mantle. Volcanic features include

the High Rock Caldera Complex [15–17] and the McDermitt Caldera [18,19]. These calderas include two of Nevada’s best-known fossil wood deposits: the Lund Petrified Forest (Figure 1) in the Black Rock Desert [20,21] and the precious opal beds at Virgin Valley (Figure 2) in Humboldt County. Other wood occurrences are well-known to collectors [22,23]. Botanical diversity in these deposits resulted from episodes of climatic change that affected local plant communities [24,25]. Nevada leaf floras have received much attention [25–30], but only a few studies have been published on permineralized cones [31] and wood [32].

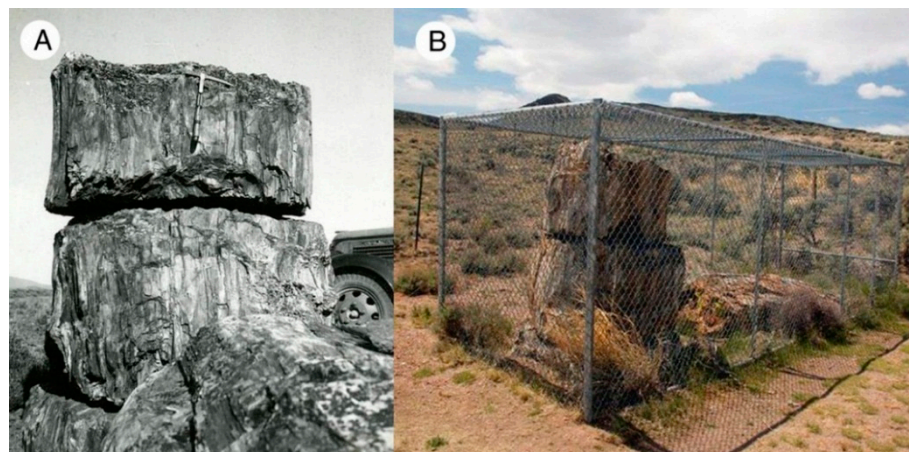


Figure 1. Lund Petrified Forest, in Washoe County, Nevada, contains remains of more than 200 stumps and logs. (A) A 1946 photo of the most prominent stump (photo courtesy of University of Nevada Reno Library Special Collections Department); (B) The same site in 2014 showing a protective fence installed by the Bureau of Land Management.

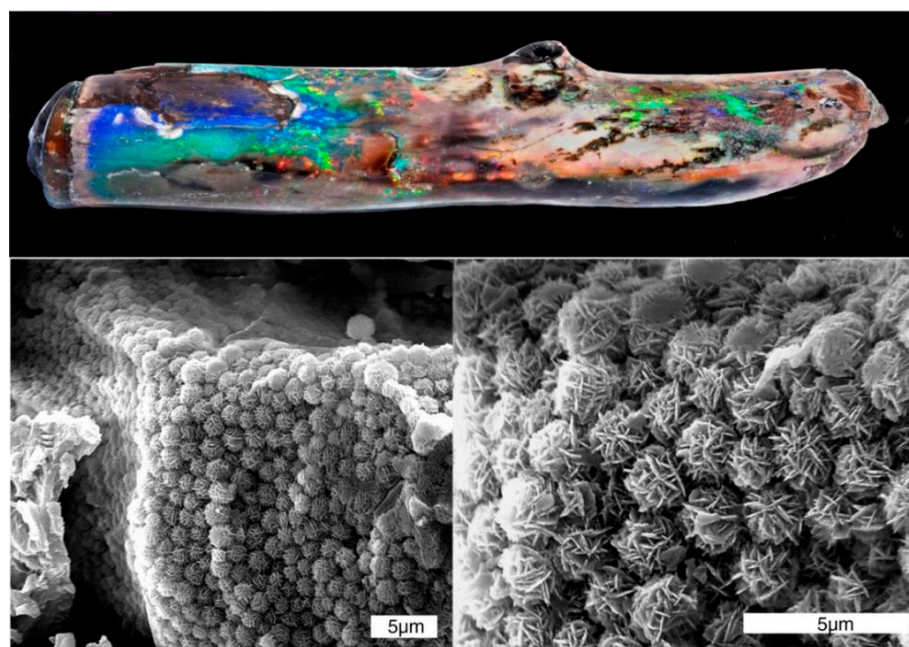


Figure 2. Twig mineralized with precious opal from Royal Peacock Mine, Virgin Valley, Nevada. SEM photos show well-ordered stacking of opal-CT lepispheres that cause the iridescent reflectance. This structural order, not the opal species, that is the cause of “fire” in precious opal; Australian precious opal is typically composed of opal-A.

3. Methods

Scanning Electron Microscopy (SEM) was performed using a Vega Tescan SEM. Samples were attached to aluminum stubs and sputter coated with palladium to provide electrical conductivity. Elemental analyses were performed using an EDAX energy-dispersive X-ray detector using Genesis software. These spectra were used to determine silica and carbon content in fossil wood, and to identify zeolite, barite, and gypsum as accessory minerals in several specimens. X-ray diffraction patterns were obtained from packed powders with a Rigaku Geigerflex diffractometer using Ni-filtered $\text{K}\alpha$ radiation. Specimens used in this study (Figure 3, Table 1) are archived at the WWU Geology Department. Specific sites are not described in this report to protect research localities from recreational collecting. Schorn *et al.* provide information on Nevada paleontology locations [33].

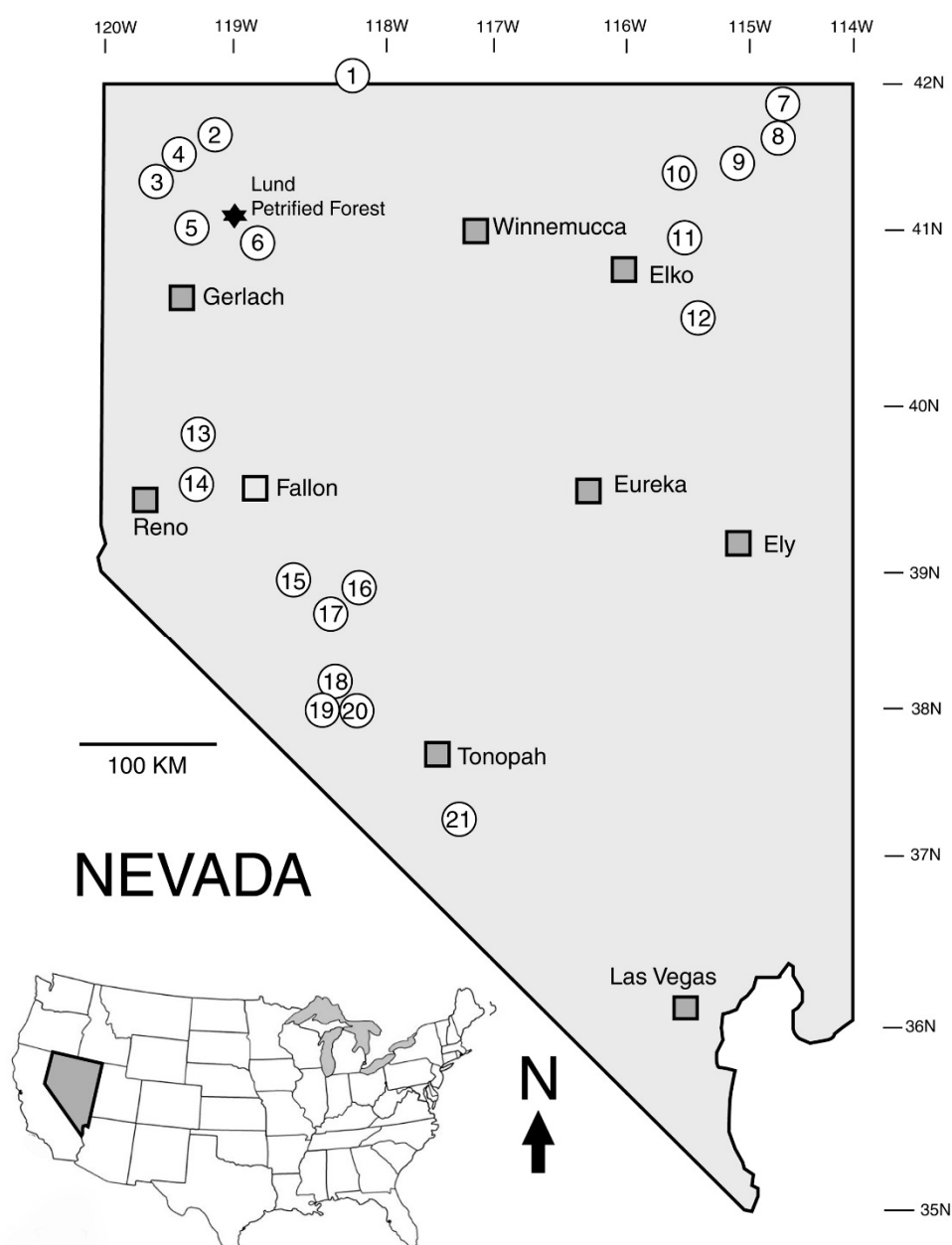


Figure 3. Localities for petrified wood specimens used in this study. See Table 1 for descriptions.

Table 1. Localities for petrified wood specimens used in this study (Figure 3).

--	Locality	County	Age	Mineralization
1	McDermitt	Humboldt Co., NV/Malheur Co./OR	Middle Miocene	Chalcedony
2	Virgin Valley	Humboldt	Middle Miocene	opal-A, opal-CT
3	Vya	Washoe	Middle Miocene	Chalcedony
4	Blowout Mountain	Washoe	Middle Miocene	opal-CT, chalcedony, quartz
5	Washoe	Washoe	Middle Miocene	opal-A
6	Black Rock Desert	Washoe	Middle Miocene	opal-CT
7	Goose Creek	Elko	Middle Miocene	opal-CT, quartz. Chalcedony
8	Texas Spring	Elko	Middle Miocene	Chalcedony
9	Tuscarora	Elko	Oligocene	Chalcedony
10	Devils Gate	Elk	Oligocene	Chalcedony
11	Hubbard Basin	Elko	Middle Miocene	Chalcedony
12	Cherry Creek	White Pine	Oligocene	Chalcedony
13	Schurz	Lyon	Middle Miocene	opal-A
14	Hazen	Churchill	Middle Miocene	opal-A
15	Rawhide	Mineral	Middle Miocene	opal-CT, quartz
16	Middlegate	Churchill	Middle Miocene	opal-CT
17	Gabbs	Nye	Lower Miocene	opal-CT, quartz
18	Sodaville	Mineral	Lower Miocene	opal-CT
19	Mina	Mineral	Lower Miocene	opal-CT
20	Miller Mountain	Mineral	Lower Miocene	opal-CT
21	Stonewall Pass	Nye	Lower Miocene	Chalcedony

4. Forms of Silica

Silicified wood may contain any of four silica polymorphs, forms of SiO_2 that have different crystallinity. These forms include opal-A (amorphous), opal-CT (incipient crystallization of cristobalite and tridymite), chalcedony (micro-fibrous quartz), and microcrystalline quartz. Opal-A commonly encrusts and permeates wood in modern hot springs, but it rarely been reported in petrified wood. However, opal-A is present at several Nevada Late Tertiary locations. “Opalized” wood usually consists of opal-CT. “Agatized” wood, the variety most prized for lapidary purposes, is mineralized with chalcedony. Less commonly, silicified wood contains microcrystalline quartz.

These silica polymorphs can be recognized by a variety of analytical methods, although no single method provides reliable characterization. X-ray diffraction (Figure 4) provides structural information, with two major limitations. Pure opal-A can be recognized by the absence of diffraction peaks, but the presence of this amorphous silica is not evident when other crystalline phases are present. Opal-CT yields a distinctive weak diffraction pattern, but quartz and chalcedony usually cannot be distinguished, because chalcedony is structurally a fibrous variety of cryptocrystalline quartz intergrown with varying amounts of moganite, a monoclinic SiO_2 polymorph.

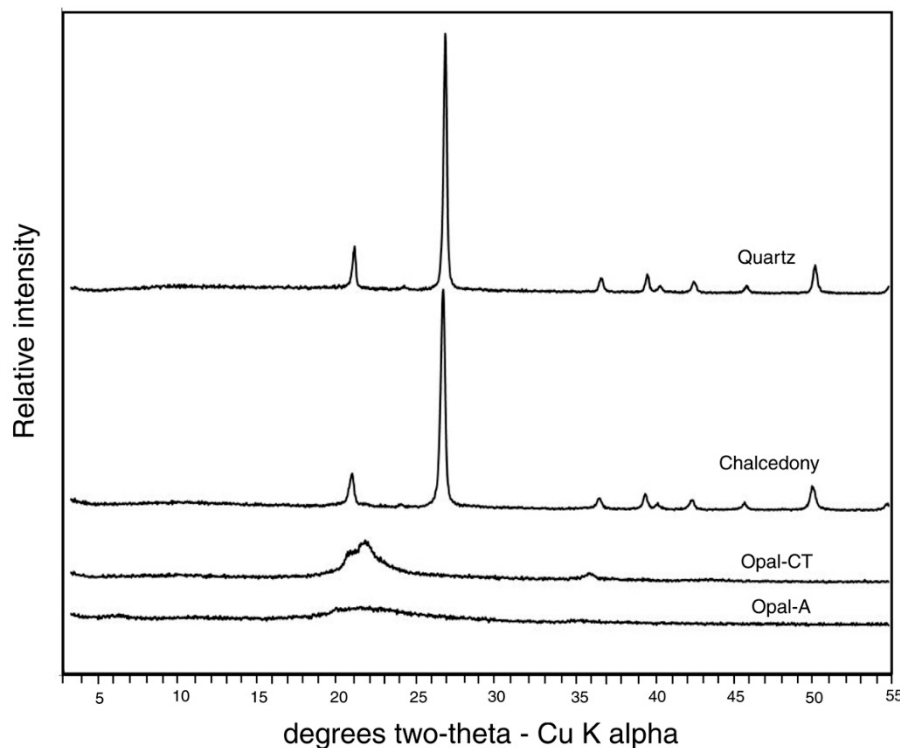


Figure 4. X-ray diffraction patterns of silica polymorphs in silicified wood.

Polarized light optical microscopy is useful for identifying quartz and chalcedony, but is seldom reliable for distinguishing opal-A from opal-CT. Higher magnifications available the scanning electron microscope are useful for discerning these silica polymorphs. Secondary electron images primarily show topography. Opal-A can be recognized as smooth-surfaced lepispheres, with individual diameters in the range of 0.5–2 microns (Figure 5A–C), and as smooth-surfaced botryoidal encrustations (Figure 5D). Opal-CT commonly exists as tabular microcrystals (Figure 6). Both varieties of opal may also occur as porous or vitreous masses. Opal-A has seldom been reported in fossil wood, but this amorphous material is fairly common in Nevada specimens. Opal-A is a major constituent of siliceous hot spring deposits, and the presence of this mineral in wood from Nevada caldera deposits is perhaps related to warm groundwater temperatures caused by local volcanism. Opal of both types is usually considered to represent an early stage in the silicification process, but an Eocene Texas locality has been reported where opal-CT is inferred to have been produced during weathering of quartz-mineralized wood [34].

Chalcedony often appears as a vitreous solid mass that may preserve anatomical details as color variations visible in transmitted light optical microscopy (Figure 7E,F). At high magnification, the fibrous structure of chalcedony may be visible (Figure 7A,B). Anatomical structure may be visible in SEM images in specimens where intercellular spaces have not been mineralized (Figure 7C). Chalcedony may also form layers lining cavities or fractures (Figure 7D).

Quartz can be recognized as hexagonal crystals. These usually occur as coatings on fracture surfaces or fillings in cavities (Figure 8). Development of euhedral crystals requires open space. When quartz is present in Nevada specimens, microtextures suggest that the mineral was precipitated as a late-stage hydrothermal precipitate, not as a primary component of petrification. In other regions, quartz crystallization has sometimes been interpreted as a primary stage in wood petrification [6,10,35,36].

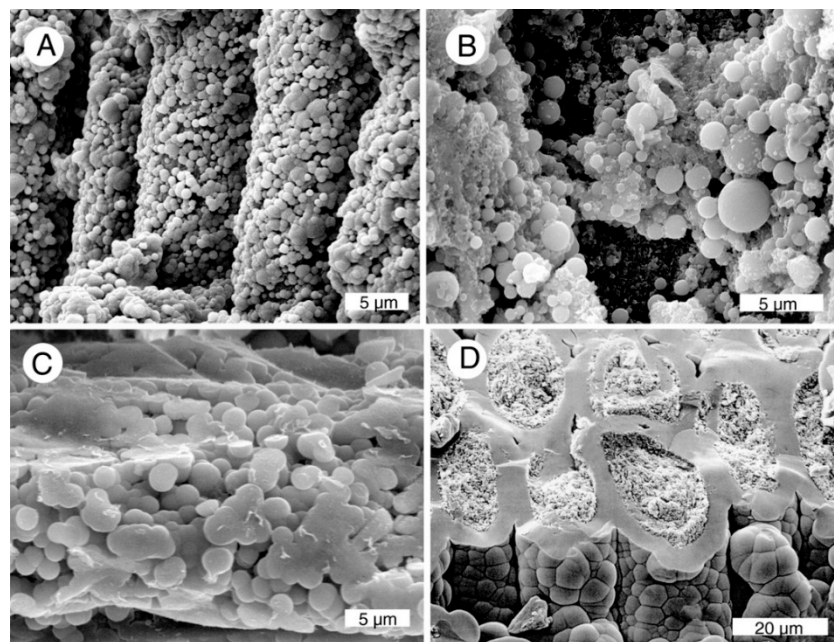


Figure 5. Examples of opal-A. (A) Tracheids coated with very small lepispheres, Location 2 (section 27 opal claim); (B) Lepispheres of varying diameters, Location 13; (C) Single tracheid mineralized with opal-A, location 14; (D) Oblique tangential view showing cell walls mineralized with botryoidal opal-A, lumina filled with porous opal-A, location 5.

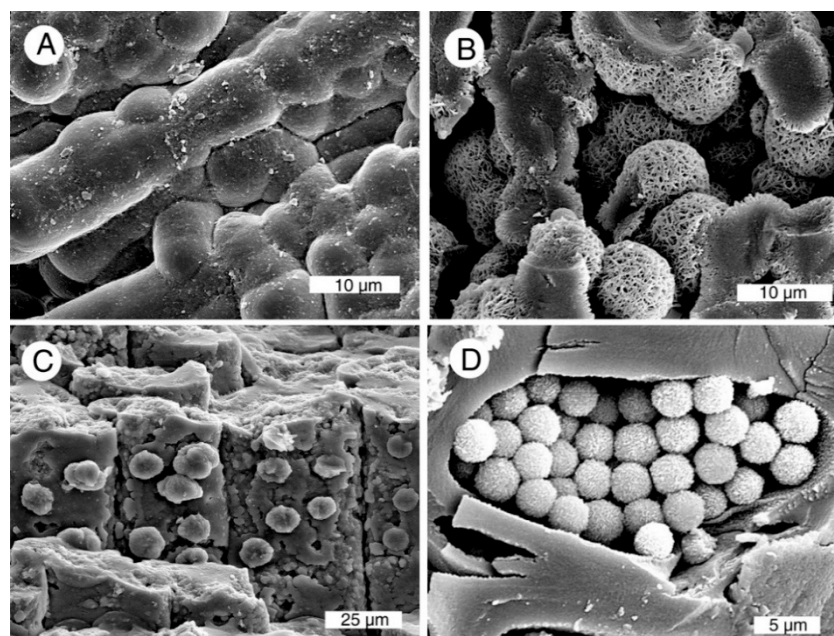


Figure 6. Examples of opal-CT. (A) Tracheids coated with microcrystalline opal, location 20; (B) Opal-CT lepispheres showing networks of tabular crystals, location 2 (Pandora opal mine); (C) Tracheids mineralized with fine-grained opal-CT, showing prominent internal casts of pit apertures. Intercellular spaces are unmineralized, locality 16; (D) Crystalline lepispheres of uniform diameter filling a single tracheid with carbonized cell walls, location 2 (Royal Peacock opal mine).

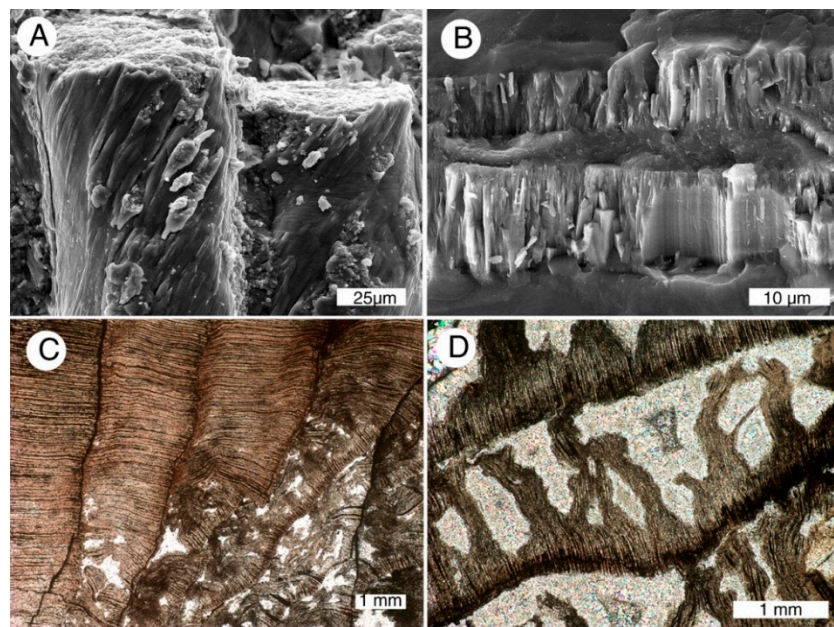


Figure 7. Examples of chalcedony. (A) Tracheids with cell walls mineralized with solid chalcedony, lumina filled with granular chalcedony; (B) Fibrous structures are, locality 10; (C,D) Transmitted light view of transverse silicified wood showing disordered structure caused by decay. Openings between permineralized cells are filled with chalcedony, location 7.

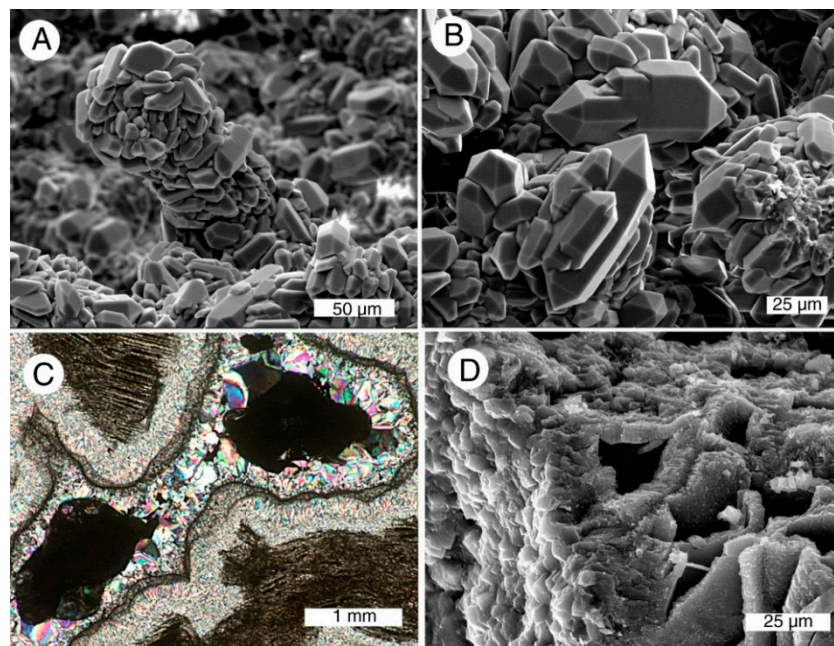


Figure 8. Examples of quartz. (A) Quartz crystals coating a single tracheid, location 6; (B) Euhedral quartz on transverse surface, location 6; (C) Polarized transmitted light view of opal-CT wood, with rot pockets containing microcrystalline chalcedony overgrown by quartz crystals. Central cavities remain open, location 7; (D) Oblique transverse view of opal-CT mineralized wood, showing layer of crystalline quartz coating surface of a fracture, location 15.

5. Anatomical Preservation

Preservation of cellular detail is highly variable among specimens from different localities, and even among individual specimens from a single locality. Anatomical preservation is related to the rate of mineralization vs. the rate of tissue degradation. Limb casts result when opal or chalcedony is deposited within a void left by a twig that has been completely destroyed, leaving only a mold in volcanic or sedimentary rocks. More commonly, gradual mineralization occurs in tissue that is simultaneously experiencing microbial degradation. Some Nevada specimens show evidence of this degradation (Figures 7C,D and 8C). However, anatomical details are commonly well-preserved. During the life of a plant, a primary function of wood is the conduction of nutrient-bearing water, and after death and burial this conductive architecture favors petrification. Groundwater is readily absorbed by tracheids, and transmitted from cell to cell by circular pits. The resulting permineralization may replicate cellular anatomy with high fidelity (Figure 9).

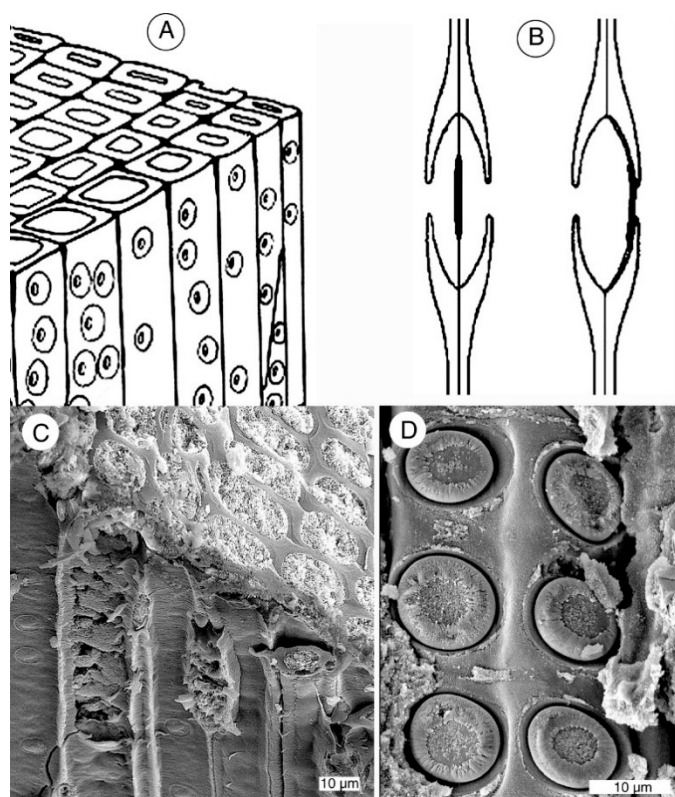


Figure 9. Wood anatomy. (A) Tracheids are parallel cells that provide fluid conduction, being laterally connected by circular pits; (B) Each pit contains a circular plate (torus) supported by a thin membrane. The torus allows the pit to open or close depending on the fluid pressure or vapor pressure of adjacent cells; (C) Oblique radial view of wood silified with opal-CT, locality 2 (Royal Peacock opal mine); (D) High magnification radial view of opal-CT wood showing details pf pit anatomy, locality 2 (Norita opal mine).

6. Results

The preceding figures illustrate the range of mineral compositions and textures present in Late Tertiary woods from Nevada localities. These photographs were selected as representative examples

from more than 500 SEM photos made from specimens from 21 different localities. Figures 5–8 show features observed in multiple specimens, commonly including specimens from at least two localities. The data have several implications for understanding how petrification occurs.

Once wood has been complexly mineralized, the original mineralization sequence is seldom evident. The Late Tertiary localities in this study include many specimens that are in early or intermediate stages of petrification. Nevada specimens provide clear evidence that wood silicification does not proceed along a single pathway. Even at a single locality, mineralogy may vary among individual specimens, or even within a single specimen. Indeed, mineralization may vary from one cell to the next. Despite these variations, some general compositional trends can be observed at wood from various localities. As a result, evidence from Nevada petrified wood provides important new insights into the silicification process.

Observations and interpretations are summarized as follows:

6.1. Silicification Commonly Begins with Precipitation of Silica within Cell Walls, with Lumina Remaining Unmineralized (Figure 10)

Mineralization processes are related to anatomical structure. Because fluid transport is a primary function of this stem tissue, tracheids readily allow groundwater to permeate buried wood. The typical first step in petrification is precipitation of silica within cell walls, facilitated by the affinity of lignin and hemicellulose for silica [37]. Silicified cell walls and empty lumina are very common features of Nevada Late Tertiary wood. Presence of silica in cell walls can be recognized by Si peaks in X-ray fluorescence spectra (SEM/EDS analysis), and by visual evidence of silica polymorphs at high magnification.

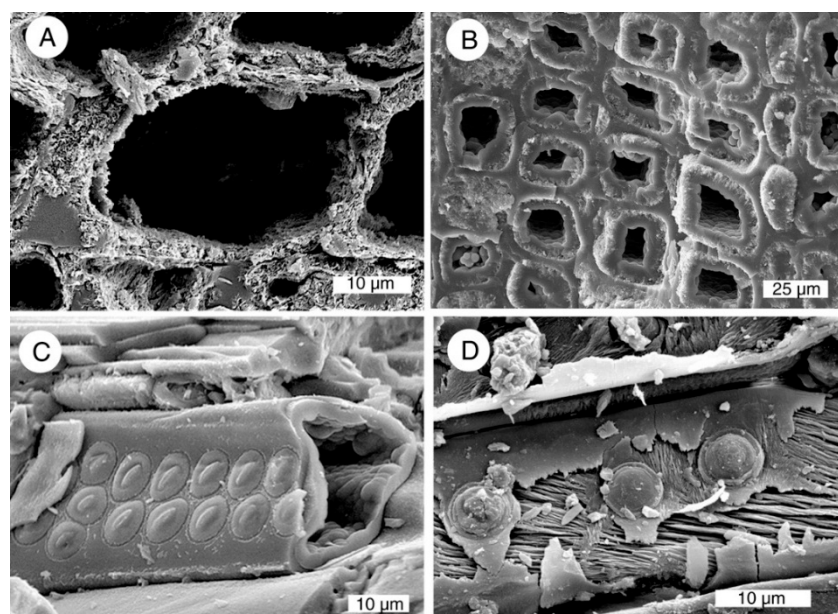


Figure 10. Empty lumina in early-stage silicified wood. (A) Opal-CT, transverse view, locality 2 (Rainbow Ridge opal mine); (B) Opal-A, transverse view, cell lumen with botryoidal lining, locality 5; (C) Single tracheid mineralized with opal-A, showing well-preserved pits, locality 14; (D) Opal-CT, radial view of single tracheid showing replication of pit apertures, multi-layered nature of cell wall, locality 6.

Subsequent mineralization occurs when silica is deposited in cell interiors (lumina), vessels, spaces between adjacent cells, and voids caused by decay or insect damage. Some Nevada localities contain wood with lumina filled with porous opal (Figures 5D and 11). The sequence of mineralization is uncertain for these specimens, but they may provide evidence that precipitation of opal can sometimes occur in cell lumina very early in the silicification process. This porosity allows the possibility of later penetration of mineral-bearing groundwater.

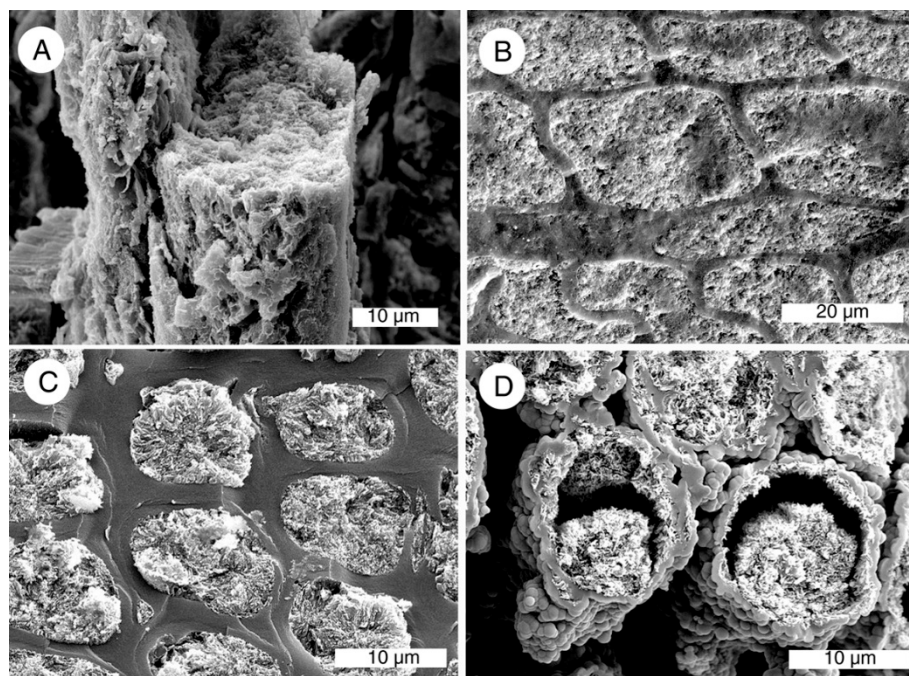


Figure 11. Porous opal in cell lumina. (A) Opal-CT, location 2 (Norita opal mine); (B,C) Opal-CT, vitreous cell walls with porous opal filling lumina, location 16; vitreous cell walls with porous opal filling lumina, location 2 (Rainbow Ridge opal mine); (D) Opal-A, botryoidal coatings on cell walls, with a thin porous interior layer, and porous partial filling of lumina, locality 2 (Section 27 opal claim).

6.2. Opal-A, Opal-CT, and Chalcedony May Be Present in Massive Form (Figures 11C and 12)

SEM secondary electron images predominately show surface topography, and silica minerals are most likely to show characteristic features when these materials border open spaces, allowing three-dimensional expression of structural characteristics. Commonly, silica is present in smooth-textured porcelain-like form, as seen in SEM images. However, many massive specimens contain local regions that have topography useful for recognizing silica phases. X-ray diffraction also provides useful information for distinguishing between silica polymorphs. The results in this study indicate that opal-A, opal-CT, and chalcedony may occur in vitreous form. Although vitreous regions may appear relatively featureless in SEM images, color variations may reveal anatomical details when the specimens are examined by optical microscopy (Figure 7C,D).

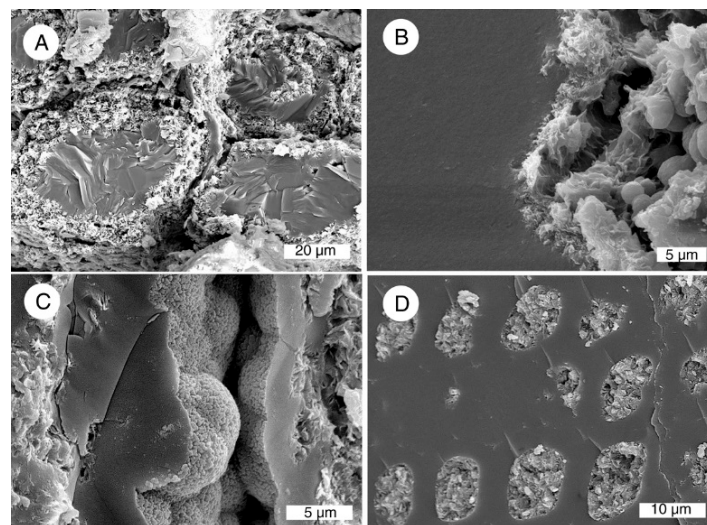


Figure 12. Massive opal. (A) Opal-CT, transverse view, cell walls mineralized with porous opal, lumina with massive filling, locality 2 (Rainbow Ridge opal mine); (B) Wood mineralized with vitreous opal-CT, microcrystalline textures visible only in open voids, locality 2 (Toni opal mine); (C) Opal-CT, radial view of a tracheid showing massive cell walls, with botryoidal microcrystalline texture visible on surfaces facing partially empty lumen, locality 2 (Rainbow Ridge opal mine); (D) Opal-CT, transverse view, massive cell walls, lumina with porous opal filling, locality 2 (Toni opal mine).

6.3. Intercellular Spaces Commonly Remain Unmineralized (Figure 13)

The exchange of silica-bearing groundwater occurs relatively easily among tracheids because of the presence of inter-cellular pits (Figure 9). Spaces between tracheids are less likely to be exposed to groundwater, which may explain why these spaces commonly remain unmineralized in Late Tertiary wood, even though cell walls and lumina are well-silicified.

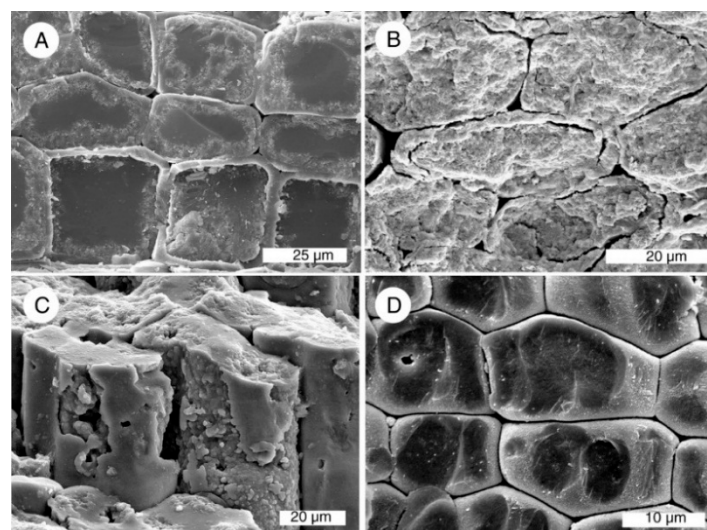


Figure 13. Open intercellular spaces in opal-CT wood. (A) Transverse view, locality 2 (Bonanza opal mine); (B) Transverse view, locality 2 (Norita opal mine); (C) Oblique radial view, locality 16; (D) Transverse view, locality 2 (Rainbow Ridge opal mine).

6.4. Mineralization May Be Different among Individual Cells within a Single Small Specimen (Figure 14)

One of the most notable characteristics of Nevada Late Tertiary woods is the wide variability of mineralization. Mineralogy may vary among individual specimens, or even among adjacent cells.

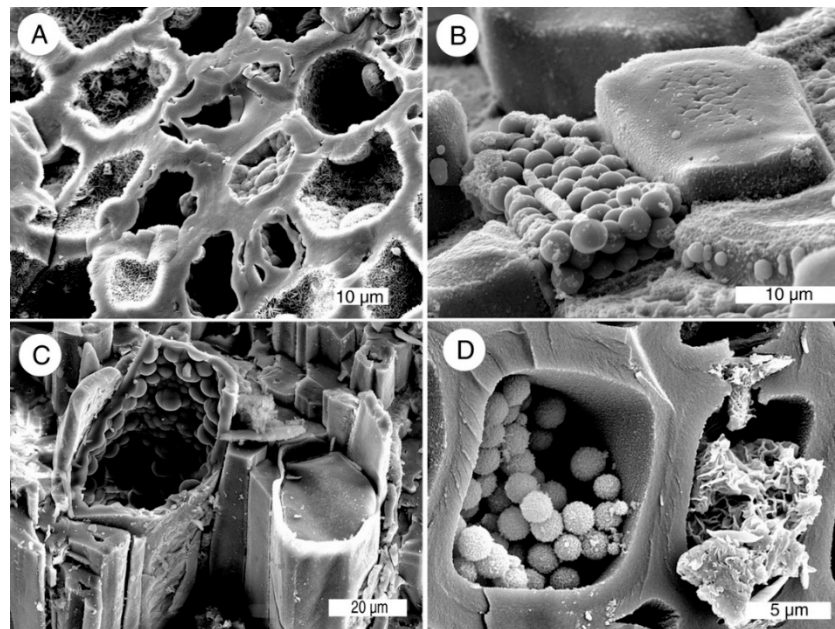


Figure 14. Cell-by-cell variability in mineralization. (A) Opal-Ct, transverse view, showing individual cells with botryoidal linings, continuous microcrystalline coatings, and microcrystalline hemispheres, locality 2 (Cessily-Ann opal mine); (B) Opal-CT, transverse views of adjacent tracheids mineralized with packed lepispheres and with solid opal. Locality 2 (Cessily-Ann opal mine); (C) Opal-A, tracheid containing botryoidal lining adjacent to tracheid with solid filling, locality 14; (D) Transverse view of carbonized cells (identified because of strong C peaks and no Si peaks in SEM.EDS spectra). One cell is partially filled with loosely-packed opal-CT lepispheres; the adjacent cell contains crinkly clay minerals, locality 2 (Royal Peacock opal mine).

The Virgin Valley Formation (locality 2) provides an excellent example. Wood is preserved in middle Miocene lacustrine sediments having a total stratigraphic thickness of approximately 300 m [38–41]. The middle zone of the formation varies in thickness from 58 to 85 m, and silicified twigs and occasional logs are found in random throughout this interval. Nearly a century of opal mining has resulted in numerous excavations within these strata; more than 200 specimens were obtained for this study, collected from the major opal mines and many smaller claims. Virgin Valley specimens are illustrated in many of the figures. Some of the best stratigraphic exposures occur at Royal Peacock Mine, where a 2 m thick wood-bearing section is exposed over a lateral distance of more than 100 m. Within this single horizon, fossil wood is abundant, including carbonized wood, ordinary opal-CT wood, and the rarest and most-prized material: “fire opal”, wood mineralized with well-ordered opal-CT lepispheres (Figure 2). Mineralogy may be variable within a single limb, and even from one cell to the next.

6.5. Carbonized Wood Is Unlikely to Become Silicified (Figure 15)

Wood buried in an anaerobic environment (e.g., impervious clay) may be protected from microbial degradation, preserved in an unmineralized state [42,43]. Carbonized wood specimens were observed at only one locality, the Royal Peacock opal mine at Virgin Valley (locality 2). These specimens commonly consist of organic tissue that had been reduced to carbon, with later precipitation of opal-CT lepispheres or clay minerals in some of the lumina. These siliceous minerals are not bonded to the adjacent carbonaceous cell walls.

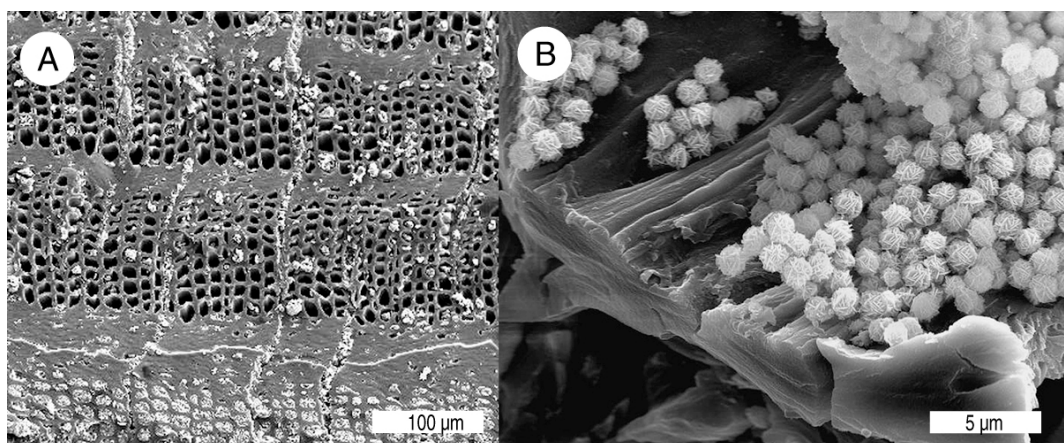


Figure 15. Partially carbonized wood showing three annual ring pairs. **(A)** Transverse view of wood with carbonized cell walls, individual cells mostly empty in two early-wood annual rings, porous opal in cells in one early-wood ring (lower part of photo); **(B)** High magnification view of cell containing opal-CT lepispheres partially filling a carbonized tracheid. Locality 2 (Royal Peacock opal mine).

6.6. Non-Silica Minerals May Be Present (Figure 16)

If groundwater contains other components besides silica, other minerals may be precipitated during petrifaction. At Virgin Valley, zeolites are a common accessory mineral, typically occurring in cells in the outer regions of wood where chemical breakdown of tephra provide a source of ions to recombine as zeolites in cell lumina. Intergrowths of zeolite and opal-Ct demonstrate that the two minerals were forming contemporaneously (Figure 16A,B). At other sites, gypsum (location 16) and barite (location 11) were observed as accessory minerals (Figure 16C,D). The intergrowth of opal-CT and zeolite are evidence that these minerals were concurrently precipitated. Barite and gypsum appear to have formed on silicified tissue as a result of secondary mineralization.

6.7. Primary Precipitation versus Diagenetic Transformations

Remaining observations relate to the common belief that wood silicification follows a transformational sequence, where opal is the initial silica phase, with chalcedony and quartz originating as successive transformations during long burial [44–47]. Evidence for this hypothesis is largely circumstantial. Diagenetic transformation of opal-A→opal-CT→quartz is well-documented for two geologic environments: biogenic sediments [48–56] and siliceous hot spring sinter [57–67].

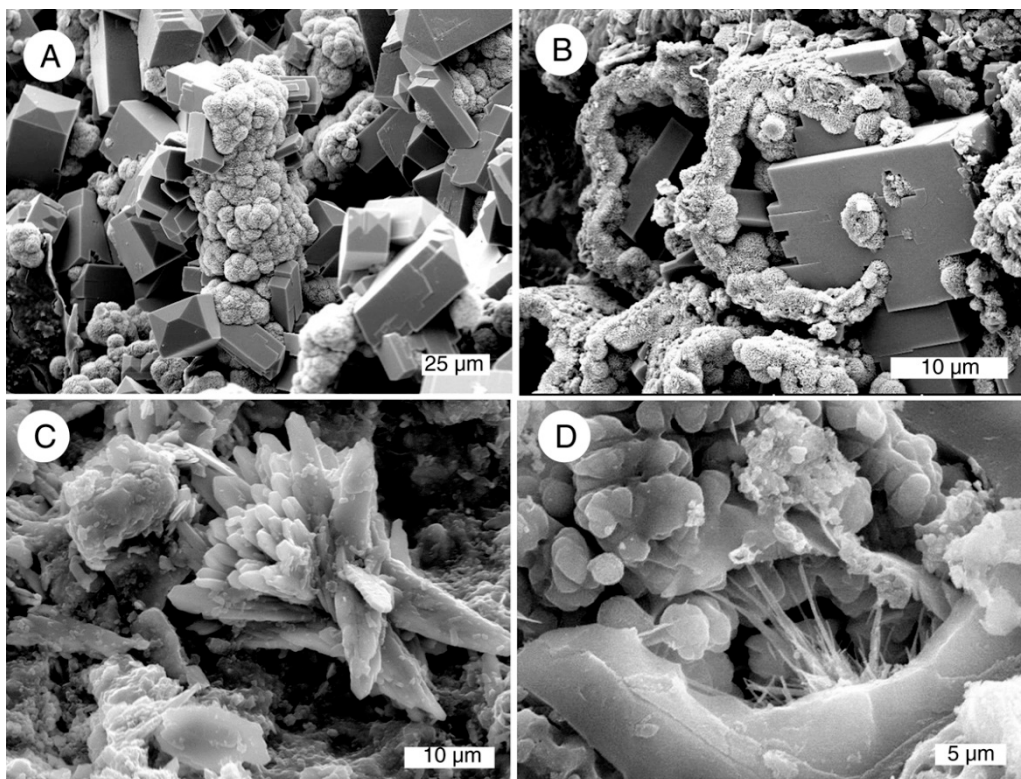


Figure 16. Non-silica mineral inclusions in silicified wood. (A) Oblique transverse view showing tracheids encrusted with botryoidal opal-CT, intergrown with blocky zeolite crystals derived from alteration of the tuffaceous matrix, locality 2 (Rainbow Ridge opal mine); (B) Transverse view showing cell walls mineralized with opal-CT, intergrown with zeolite crystals, locality 2 (Royal Peacock opal mine); (C) Radiating barite crystals on chalcedony mineralized wood, locality 11; (D) Acicular gypsum microcrystals in opal-CT wood, locality 20. Non-silica minerals were identified from SEM/EDS spectra.

If gradual mineral transformation is a common process during petrifaction, it would seem likely that many deposits would reveal petrified wood that contains both opal and chalcedony. However, this association is surprisingly rare. Opal-CT and chalcedony coexist in late Eocene specimens from the Florissant, Colorado fossil forest, but these silica phases appear to have been formed during separate stages of mineral deposition, not as a transformative sequence [68]. Nevada specimens provide further evidence that silicification may proceed along a variety of pathways.

6.8. Multiple Silica Phases May Coexist as a Result of Successive Episodes of Precipitation (Figure 17)

Some individual Nevada wood specimens contain several forms of silica that appear to have formed in separate precipitation events. One example is the presence of opal-A or opal-CT in different physical forms (Figure 17A,C). Quartz and opal-CT typically coexist because quartz was deposited in fractures or open other spaces in wood that had previously been permineralized with opal. Evidence for this hypothesis comes from the presence of quartz along fracture planes that crosscut botanical structures, a geometry that can only occur if the wood has been rendered brittle because of mineralization.

Based on comparison to geodes and vein deposits, in these circumstances, mineral deposition may be related to dissolved silica concentrations. High silica concentrations favor rapid precipitation of opal or

chalcedony; low silica concentrations favor precipitation of quartz, when slow crystallization rates allow formation of well-ordered lattices and open spaces allow development of terminated crystals. Quartz has been observed as a primary agent of petrifaction at a few locations in other regions, e.g., the Eocene Yegua Formation of Texas [34] and Cretaceous and Paleocene wood in Alabama [69]. Like crystalline quartz, chalcedony may occur as a filling material in vugs and fractures, (Figure 17D); chalcedony is the main constituent of “agatized” wood at locations 1, 3, 9–12, and 21.

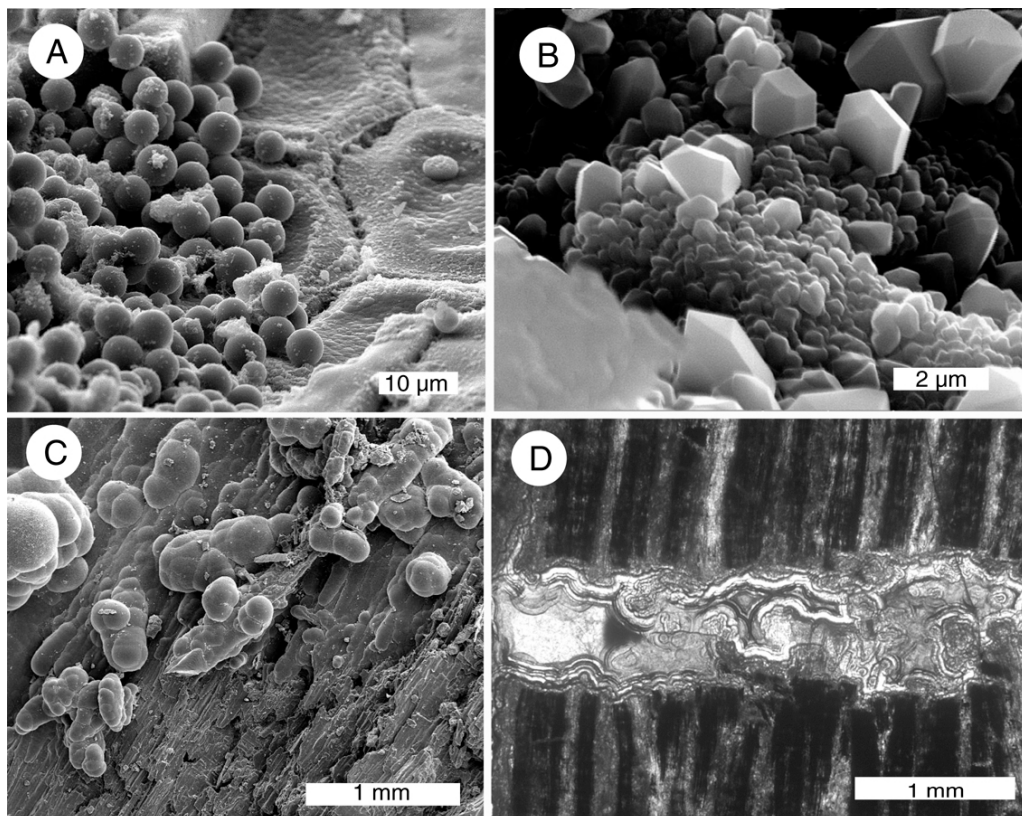


Figure 17. Silicified wood containing multiple primary silica phases. **(A)** Opal-A lepispheres precipitated on solidly-mineralized cells, transverse view, locality 2 (Cessily-Anne opal mine); **(B)** Euhedral quartz crystals formed on wood mineralized with opal-CT, locality 17; **(C)** Large-diameter botryoidal opal-CT coating wood permineralized with fine-grained opal-CT, locality 6; **(D)** Opal-CT wood, with transverse fracture filled with multi-layered chalcedony, locality 4.

6.9. Relict Textures Suggest Opal May Transform to Chalcedony (Figure 18)

Opal and chalcedony rarely occur together in Nevada specimens, though chalcedony mineralized wood is very common. Several locations yielded specimens where chalcedony appears to preserve relict lepispheres that are evidence of the original opal mineralization. This mode of occurrence contrasts the chalcedony that appears to have formed as a primary mineral (e.g., Figures 8C and 17D).

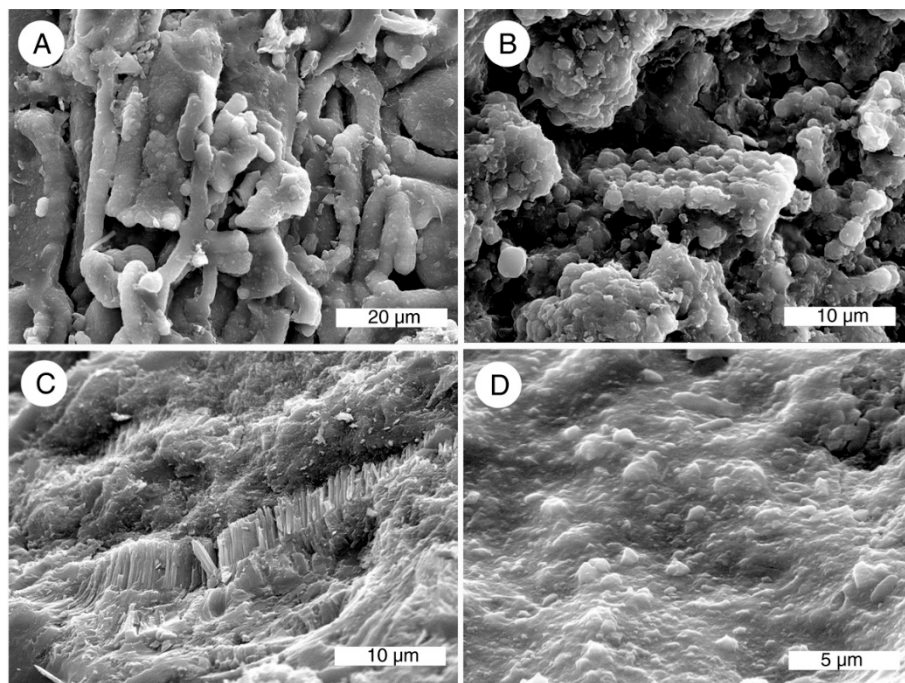


Figure 18. Evidence of diagenetic transformation of silica. (A) Tracheids coated with chalcedony, a texture common in opalized wood (e.g., Figure 6A); (B) Chalcedony showing structure reminiscent of opal lepispheres (e.g., Figures 5 and 6); (C) Chalcedony showing fibrous crystalline habit. (A–C) all from locality; (D) Chalcedony mineralized wood showing relict hemispherical texture typical of opal, locality 11.

7. Discussion

Nevada petrified wood localities provide an important opportunity for studying the fossilization process in Late Tertiary wood, where the sequential steps in the mineralization process can be directly observed, rather than attempting to reconstruct early mineralization sequences by inference from wood from older deposits that may have had a complex diagenetic history.

Nevada Late Tertiary specimens yield information that is markedly different from some previous hypotheses based on studies of Paleozoic and Mesozoic wood. For example, Nevada fossil wood commonly has permineralized cell walls, with lumina remaining empty (Figure 10). This observation is consistent with the experimental studies [37] that show silica is actively precipitated in cell walls because of the chemical affinity of lignin and cellulose for silicic acid. In contrast, the empty lumina conflict with hypotheses that assert silicification begins with precipitation of porous silica within cell lumina [11,70–73].

Another discrepancy involves the possibility of quartz as a primary agent of silicification. In Permian wood from Chemnitz, Germany, cell walls contain quartz crystals and cell lumina are filled with cryptocrystalline silica. This mineralogy has been interpreted as evidence that quartz precipitated on oriented cellulose fibrils within the cell wall, and that larger quartz crystals grew in open spaces [11]. In Nevada specimens, crystalline quartz was only observed as a secondary mineral precipitated in fractures and void spaces, though in these locations quartz crystals may coat individual fibers that face the open areas (e.g., Figure 8A,B). Cryptocrystalline quartz (chalcedony) in cell walls appears to have formed from a process of diagenetic transformation from an opaline parent material, but chalcedony in lumina, vessels, and rot cavities sometimes originated as a primary precipitate. Though chalcedony has not yet

been synthesized as a primary silica phase in laboratory, this silica polymorph commonly occurs as a primary phase in geode deposits from many locations in North America (example: Figure 19A).

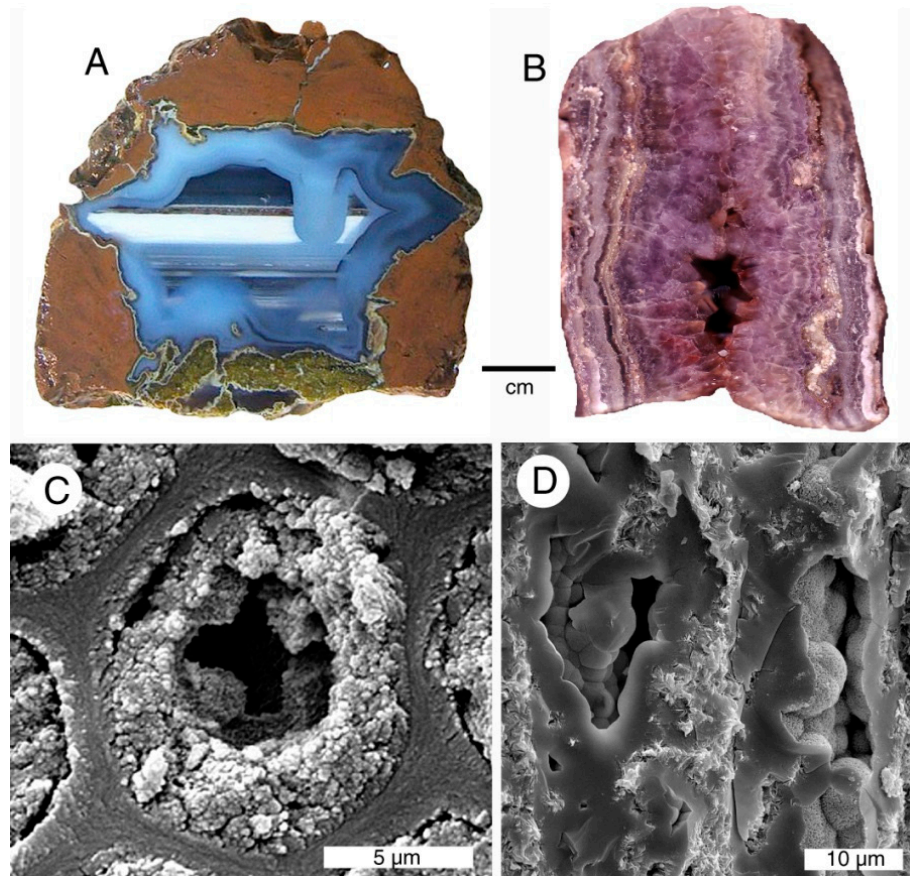


Figure 19. (A) This “thunderegg” nodule from central Oregon, USA originated when a vesicle in welded tuff became filled with silica minerals that precipitated after groundwater entered the cavity via fractures in the host rock. The star shape shows the entry points for the silica-bearing fluid. The first stage of mineralization was deposition of light blue gray chalcedony around the periphery of the cavity, including a stalactitic shape at upper right. Later silica precipitation produced successive horizontal layers of dark translucent chalcedony, with a prominent white layer of common opal; (B) Vein from Arizona, USA shows layers of crystalline quartz (amethyst variety) parallel to the side walls, with well-terminated crystals on interior surfaces of a midline cavity; (C) Transverse view of fossil wood from locality 2 (Rainbow Ridge opal mine). Cell walls mineralized with vitreous opal separate each tracheid. The lumina are partially filled with granular opal-CT. The structure resembles geodes, where minerals precipitate on the side walls of a circular chamber; (D) Radial view of two tracheids from location 2 (Rainbow Ridge opal mine). Botryoidal layers of opal-CT coat the inside surfaces of cell walls, with the central interior remaining empty. This architecture is reminiscent of veins, where mineralizing fluids enter a linear fracture. The fossil wood thus contains a combination of geode and vein characteristics, originating from multiple stages of mineral precipitation in an elongate open space having a circular cross-section.

Incipient silicification involves organic templating within cell walls, but subsequent episodes of silicification mostly involve open space filling. The most useful analogy may be the precipitation of silica in geodes and veins, where silica is deposited in successive layers within empty spaces in a host rock [74]. For vein deposits, these spaces are created by brittle fracturing. For geodes, the spaces may be vesicles in a volcanic rock, or erosional spaces in a sedimentary rock. Mineralization occurs when groundwater enters via fractures or porosities in the host rock. This physical setting is similar to the absorption of groundwater by buried wood, the main difference being the relative sizes and shapes of the open spaces. Tracheids and vessels typically have diameters of 50 microns or less, with tube-like architecture. Variations in mineralogy within these cells may result from microhydrology. The flow of silica-bearing groundwater into tracheids and vessels is influenced by anatomical characteristics. Damage to pits or cell walls may inhibit permeability. Other preservational factors may also play a role, e.g., crushing of tissue, or local decay. These structural variations may explain specimens of the type illustrated in Figure 14, where neighboring cells have differing mineralogy.

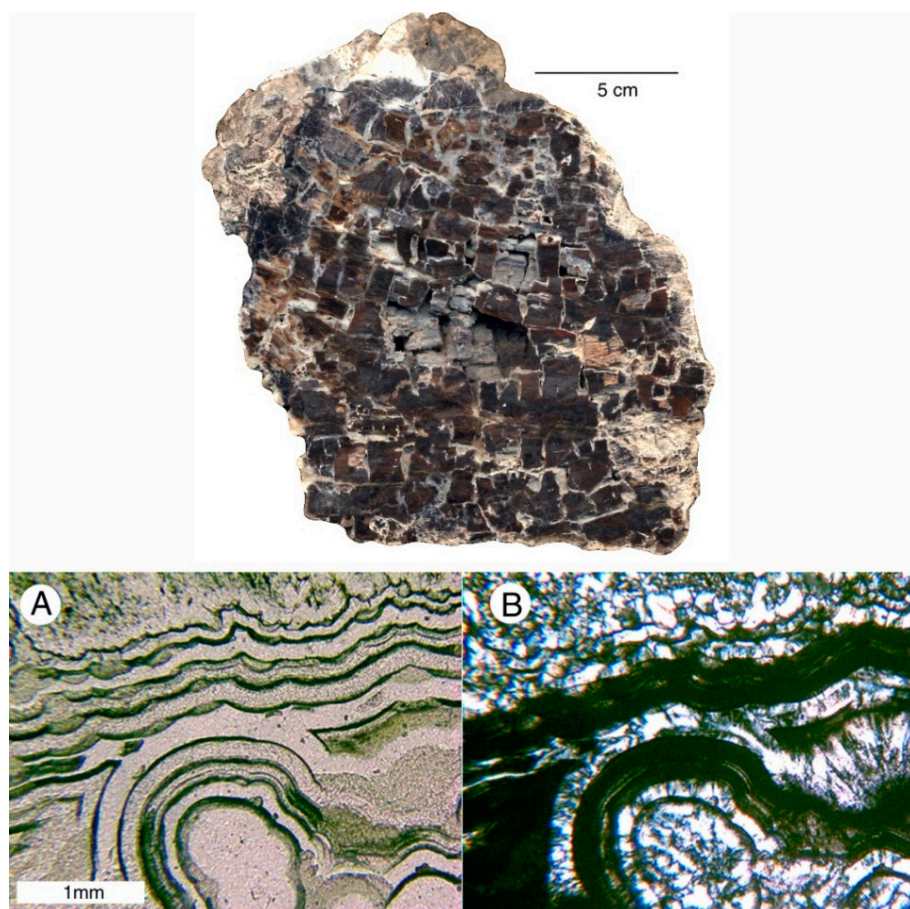


Figure 20. In geodes, veins, and silicified wood, silica minerals may occur in alternating layers. This photomicrograph pair shows minerals in a decay space in fossil wood from locality 4. (A) Ordinary transmitted light, showing dark opal-CT and colorless chalcedony; (B) polarized light, revealing chalcedony as bright birefringent areas.

The geode/vein analogy accounts for many instances where a single fossil wood specimen contains several different silica polymorphs. This phenomenon is common in geodes, where successive episodes of mineralization may precipitate opal, chalcedony, or quartz, sometimes in interlayered form

(Figures 19 and 20). Veins may likewise be filled with several different minerals precipitated in separate events. Physical and chemical factors that control mineral formation may include the concentration of dissolved silica, pH, and temperature. Crystalline quartz is commonly present in geodes and veins as a primary product, not derived from an earlier silica precursor. Well-terminated quartz crystals are likely to form when there is empty interior space to allow unrestricted growth.

8. Conclusions

The most important inference that can be made from Nevada specimens is that wood silicification does not follow a single pathway. Instead, mineralization may result from a diverse variety of processes, including successive stages of silica precipitation under varying geochemical conditions, and diagenetic transformation of opal to chalcedony.

Acknowledgments

This study greatly benefitted from permission from property owners to visit opal mines at Virgin Valley, Nevada in 2004. I particularly thank Joy and Harry Wilson (Royal Peacock Mine), John Church (Swordfish Mining), Glenn Hobson (Rainbow Ridge Mine), and Pat and Scott Ryals (Opal Negra Mine). Informal conversations with mine owners were a valuable source of geologic and historical information regarding the opal deposits. Nevada petrified wood specimens were contributed by many individuals. Richard Rantz, Jim Mills, and Patricia Caplette were particularly generous. Western Washington University Scientific Technical Services staff members Erin Macri and Charles Wandler deserve special credit for their expertise in maintaining the scanning electron microscope at Western Washington University, and for providing many hours of access to this instrument. I thank Thomas Yancey and Chris Ballhaus for providing detailed manuscript commentary, supplementing helpful contributions from three anonymous reviewers. This paper is dedicated to the late Howard Schorn (1933–2013). A Museum Associate at University of California Museum of Paleontology at Berkeley, Howard Schorn was a leading expert on Nevada plant fossils who always generously shared his extensive knowledge.

Conflicts of Interest

The author declares no conflict of interest.

References

1. Akahane, H.; Furuno, T.; Miyama, H.; Yoshikawa, T.; Yamamoto, S. Rapid wood silicification in hot spring water: An explanation of silicification of wood during the Earth's history. *Sediment. Geol.* **2004**, *169*, 219–228.
2. Channing, A.; Edwards, D. Experimental silicification of plants in Yellowstone hot-spring environments. *Trans. R. Soc. Edinb. Earth Sci.* **2004**, *94*, 503–521.
3. Channing, A.; Edwards, D. Yellowstone hot spring environments and the palaeo-ecophysiology of Rhynie chert plants: Towards a synthesis. *Plant Ecol. Divers.* **2009**, *2*, 111–143.

4. Hellawell, J.; Balhaus, C.; Gee, C.T.; Mustoe, G.E.; Nagel, T.J.; Wirth, R.; Rethemeyer, J.; Tomaschek, F.; Geisler, T.; Greef, K.; *et al.* Incipient silicification of recent conifer wood at a Yellowstone hot spring. *Geochim. Cosmochim. Acta* **2015**, *149*, 79–87.
5. Dietrich, D.; Viney, M.; Lampke, T. Petrifications and wood-templated ceramics: Comparisons between natural and artificial silicification. *IAWA J.* **2015**, *36*, 167–185.
6. Menci, V.; Matysová, P.; Sakala, J. Silicified wood from the Czech part of the Intra Sudetic Basin (Late Pennsylvanian, Bohemian Massif, Czech Republic): Systematics, silicification, and paleoenvironment. *Neues Jahrbuch für Geologie und Paläontologie-Abhandlungen* **2009**, *253*, 269–288.
7. Witke, K.; Götze, J.; Rössler, R.; Dietrich, D.; Marx, G. Raman and cathodoluminescence spectroscopic investigations on Permian fossil wood from Chemnitz—A contribution to the study of the permineralization process. *Spectrochim. Acta Part A: Mol. Biomol. Spectrosc.* **2004**, *60*, 2903–2912.
8. Rössler, R. Two remarkable Permian petrified forests: Correlation, comparison, and significance. *Geol. Soc. Lond. Spec. Publ.* **2006**, *265*, 39–63.
9. Sigleo, A.C. Geochemistry of silicified wood and associated sediments, Petrified Forest National Monument, Arizona. *Chem. Geol.* **1979**, *26*, 151–163.
10. Matysová, P.; Rössler, R.; Götze, J.; Leichmann, J.; Forbes, G.; Taylor, E.; Sakala, J.; Grygar, T. Alluvial and volcanic pathways to silicified plant stems (Upper Carboniferous-Triassic) and their taphonomic and palaeoenvironmental meaning. *Palaeogeogr. Palaeoclimatol. Palaeoecol.* **2010**, *292*, 127–143.
11. Dietrich, D.; Lampke, T.; Rössler, A. Microstructure study on silicified wood from the Permian Petrified Forest of Chemnitz. *Paläontologische Z.* **2013**, *87*, 397–407.
12. Henry, C.D.; John, D.A. Magmatism, ash-flow tuffs, and calderas of the ignimbrite flare-up in the western Nevada volcanic field, Great Basin, USA. *Geosphere* **2013**, *9*, 951–1008.
13. Sawyer, D.A.; Fleck, R.K.; Lanphere, M.A.; Warren, R.G.; Brockton, D.E.; Hudson, M.R. Episodic caldera volcanism in the Miocene southwestern Nevada volcanic field: Revised stratigraphic framework, $^{40}\text{Ar}/^{39}\text{Ar}$ geochronology, and implications for magmatism and extrusion. *GSA Bull.* **1994**, *10*, 1304–1318.
14. Robinson, P.T.; Stewart, J.H. *Uppermost Oligocene and Lowermost Miocene Ash-Flow Tuffs of Western Nevada*; Bulletin 1557; U.S. Geological Survey: Reston, VA, USA, 1984.
15. Ach, J.A.; Swisher, C.C. The High Rock caldera complex nester “failed” calderas in northwestern Nevada. *EOS Trans. N. Am. Geophys. Union* **1990**, *71*, 1614.
16. Coble, M.A.; Mahoud, G.A. Initial impingement of the Yellowstone plume located in widespread silicic volcanism contemporaneous with Columbia River flood basalts. *Geology* **2012**, *40*, 655–658.
17. Coble, M.A.; Mahoud, G.A. New geologic evidence for additional 16.5–15.5 Ma silicic calderas in northwest Nevada related to initial impingement of the Yellowstone hot spot. In Proceedings of the IDP Conference Series: Earth and Environmental Science, Warwick, UK, 10–11 September 2015.
18. Greene, R.C. *Volcanic Rocks of the McDermitt Caldera, Nevada-Oregon*; USGS Open-File Report: Reston, VA, USA, 1976.
19. Rytuba, J.J. *Geology and Ore Deposits of the McDermitt Caldera, Nevada-Oregon*; USGS Open-File Report: Reston, VA, USA, 1976.
20. Murbarger, N. Our largest petrified tree: Natural history. *1953, LXII*, 466–471.

21. Erwin, D.M.; Schorn, H.E.; Smith, R.V.; Levy, L.M.; Millar, C.I.; Westfall, R.D.; King, J.C.; Moran, V.S. Nevada's buried treasure: The Lund Petrified Forest. In Proceedings of the Botanical Society of America Botany Annual Meeting, Austin, TX, USA, 13–17 August 2005.
22. Kappele, W.A. *Rock Hounding Nevada*, 2nd ed.; Morris Book Company: Guilford, CT, USA, 2011.
23. Mitchell, J.R. *Gem Trails of Nevada*, 2nd ed.; Gem Books Book Company: Baldwin Park, CA, USA, 2002.
24. Axelrod, D.I.; Schorn, H.E. The 15 Ma floristic crisis at Gilliam Spring, Washoe County, northwestern Nevada. *PaleoBios* **1994**, *16*, 1–10.
25. Axelrod, D.I. *Miocene Floras from the Middlegate Basin, West-Central Nevada*; University of California Press: Berkeley, CA, USA, 1985.
26. Axelrod, D.I. *Mio-Pliocene Floras from West-Central Nevada*; University of California Publications in Geological Sciences; University of California Press: Berkeley, CA, USA, 1956.
27. Axelrod, D.I. *The Early Miocene Buffalo Canyon Flora of Western Nevada*; University of California Publications in Geological Sciences; University of California Press: Berkeley, CA, USA, 1991.
28. Axelrod, D.I. *The Middle Miocene Pyramid Flora of Western Nevada*; University of California Publications in Geological Sciences; University of California Press: Berkeley, CA, USA, 1991.
29. Axelrod, D.I. *The Miocene Purple Mountain Flora, Western Nevada*; University of California Publications in Geological Sciences; University of California Press: Berkeley, CA, USA, 1992.
30. Wolfe, J.A. *Miocene Flora from Fingerrock Wash, Southwestern Nevada*; US Geological Survey Professional Paper; US Geological Survey: Reston, VA, USA, 1964.
31. Crabtree, D.R. *Picea wolfei*, a new species of petrified cone from the Miocene of northwestern Nevada. *Am. J. Bot.* **1963**, *70*, 1356–1364.
32. Tidwell, W.D.; Parker, L.R. *Protocyucca shadishii*, gen. et sp. nov., An arborescent monocotyledon with secondary growth rings from the middle Miocene of northwest Nevada, USA. *Rev. Palaeobot. Palynol.* **1990**, *67*, 79–95.
33. Schorn, H.E.; Bell, C.J.; Starratt, S.W.; Wheeler, D.T. *A Computer-Assisted Annotated Bibliography and Preliminary Survey of Nevada Paleobotany*; USGS Open-File Report: Reston, VA, USA, 1994.
34. Senkayi, A.L.; Dixon, J.B.; Hosner, L.R.; Cerima, B.K.P.; Wilding, L.P. Replacement of quartz by opaline silica during weathering of petrified wood. *Clays Clay Miner.* **1985**, *33*, 525–531.
35. Beauchamp, J. Structure et mode de silicification de quelques bois fossiles. *Bulletin de la Société Géologique de France* **1981**, *34*, 13–20.
36. Wiebel, R. Petrified wood from an unconsolidated sediment, Voervadsbro, Denmark. *Sediment. Geol.* **1996**, *101*, 31–41.
37. Leo, R.P.; Barghoorn, E.S. Silicification of wood. *Bot. Mus. Leafl. Harv. Univ.* **1976**, *25*, 1–47.
38. Fyock, T.L. The Stratigraphy and Structure of the Virgin Valley-Thousand Springs Area, Northwestern Nevada. Master's Thesis, University of Washington, Seattle, WA, USA, 1963.
39. Wendell, W.G. The Structure and Stratigraphy of the Virgin Valley-McGee Mountain Area, Humboldt County, Nevada. Master's Thesis, Oregon State University, Corvalis, OR, USA, 1970.
40. Brophy, J.G. Geology of the Virgin Valley-Rock Springs Table Area, Humboldt County, Nevada. Master's Thesis, Colorado School of Mines, Golden, CO, USA, 1980.
41. Zielinski, R.A. Uraniferous opal, Virgin Valley, Nevada: Conditions of formation and implications for uranium exploration. *J. Geochem. Explor.* **1982**, *16*, 197–216.

42. Yancey, T.E.; Mustoe, G.E.; Leopold, E.B.; Heizler, M.T. Mudflow disturbance in latest Miocene forests in Lewis County, Washington. *Palaios* **2013**, *28*, 343–358.
43. Bardot, M.; Pournou, A. Fossil wood from the Miocene and Oligocene epoch: Chemistry and morphology. *Magn. Reson. Chem.* **2015**, *53*, 9–14.
44. Buurman, P. Mineralization of fossil wood. *Scr. Geol.* **1972**, *12*, 1–35.
45. Stein, C.L. Silica recrystallization in petrified wood. *J. Sediment. Petrol.* **1982**, *52*, 1277–1282.
46. Scurfield, G. Wood petrifaction: An aspect of biomineralogy. *Aust. J. Bot.* **1979**, *27*, 377–390.
47. Scurfield, G.; Segnit, E.R. Petrification of wood by silica minerals. *Sediment. Geol.* **1984**, *39*, 149–167.
48. Davis, E.F. The radiolarian cherts of the Franciscan Group. University of California Press: Berkeley, CA, USA, 1918.
49. Ernst, W.G.; Calvert, S.E. An experimental study of the recrystallization of porcelainite and its bearing on the origin of some bedded cherts. *Am. J. Sci.* **1969**, *267*, 114–133.
50. Mitzutani, S. Silica minerals in the early stages of diagenesis. *Sedimentology* **1970**, *15*, 419–436.
51. Mitzutani, S. Progressive ordering of cristobalite in early stages of diagenesis. *Contrib. Mineral. Petrol.* **1977**, *61*, 129–140.
52. Murata, K.J.; Nakata, J.K. Cristobalitic stage in the diagenesis of diatomaceous shale. *Science* **1974**, *276*, 1120–1130.
53. Kastner, M.; Keene, J.B.; Geisekes, J.M. Diagenesis of siliceous oozes—I. Chemical controls on the rate of opal-A to opal-CT transformation—An experimental study. *Geochim. et Cosmochim. Acta* **1977**, *41*, 1041–1059.
54. Iijama, A.; Tada, R. Silica diagenesis of Late Tertiary diatomaceous and volcaniclastic sediments in northern Japan. *Sedimentology* **1981**, *28*, 185–200.
55. Williams, L.A.; Crerar, D.A. Silica diagenesis, II. General mechanisms. *J. Sediment. Petrol.* **1985**, *55*, 312–311.
56. Williams, L.A.; Parks, G.A.; Crerar, D.A. Silica diagenesis, I. Solubility controls. *J. Sediment. Petrol.* **1985**, *55*, 301–311.
57. White, D.E.; Thompson, G.A.; Sandberg, C.H. *Rocks, Structure, and Geologic History of Steamboat Springs Thermal Area, Washoe County, Nevada*; U.S. Geological Survey Professional Paper: Reston, VA, USA, 1964.
58. White, D.E.; Herpolous, C.; Fournier, R.O. *Gold and Other Minor Elements Associated with Hot Springs and Geysers of Yellowstone National Park, Wyoming, Supplemented with Data from Steamboat Springs, Nevada*; Bulletin 201; US Geological Survey: Reston, VA, USA, 1992.
59. Herdianita, N.R.; Browne, P.R.L.; Rodgers, K.A. Mineralogical and textural changes accompanying ageing of silica sinter. *Miner. Depos.* **2000**, *35*, 48–62.
60. Smith, B.Y.; Campbell, K.A.; Rodgers, K.A.; Brown, P.R.L. Morphologicaal changes accompanying the opal-A to opal-CT silic phase transition in silica sinters, from Orakei Korako and Te Kopia, Taupo Volcanic Zone. In Proceedings of the GSA Annual Meeting, Boston, MA, USA, 5–8 November 2001.
61. Guidry, S.A.; Chafetz, H.S. Depositional facies and diagentic alterationin a siliceous hot-spring accumulation: Examples from Yellowstone National Park, USA. *J. Sediment. Res.* **2003**, *73*, 806–823.
62. Lynne, B.Y.; Campbell, K.A.; Perry, R.S.; Browne, P.R.L.; Moore, J.N. Acceleration of sinter diagenesis in an active fumarole, Taupo Volcanic Zone, New Zealand. *Geology* **2006**, *34*, 749–752.

63. Lynne, B.Y.; Campbell, K.A.; Moore, J.N.; Brown, P.R.L. Diagenesis of 1900-year old silica sinter (opal-A to quartz) at Opal Mound, Roosevelt Hot Springs, Utah, USA. *Sediment. Geol.* **2005**, *179*, 245–278.
64. Lynne, B.Y.; Campbell, K.A.; James, B.J.; Browne, P.R.L.; Moore, J. Tracking crystallinity in siliceous hot-spring deposits. *Am. J. Sci.* **2007**, *307*, 512–641.
65. Lynne, B.Y.; Campbell, K.A.; Moore, J.; Browne, P.R.L. Origin and evolution of the Steamboat Springs siliceous sinter deposit, Nevada, USA. *Sediment. Geol.* **2008**, *10*, 111–131.
66. Lynne, B.Y.; Campbell, K.A. Morphologic and mineralogic transitions for opal-A to opal-CT in low-temperature siliceous sinter diagenesis, Taupo Volcanic Zone, New Zealand. *J. Sediment. Res.* **2004**, *74*, 562–579.
67. Lynne, B.Y.; Campbell, K.A. Diagenetic transformation (opal-A to quartz) of low- and mid-temperature microbial textures in siliceous hot spring deposits, Taupo Volcanic Zone, New Zealand. *Can. J. Earth Sci.* **2011**, *40*, 1679–1696.
68. Mustoe, G.E. Mineralogy and geochemistry of late Eocene silicified wood from Florissant Fossil Beds National Monument, Colorado. In *Paleontology of the Upper Eocene Florissant Formation, Colorado*; Meyer, H.W., Smith, D.M., Eds.; Geological Society of America Special Paper 435; Geological Society of America: Boulder, CO, USA, 2008; pp. 127–140.
69. Cahoon, E.J. *Paraphyllanthoxylon alabamense*—A new species of fossil dicotyledonous wood. *Am. J. Bot.* **1972**, *59*, 5–11.
70. Furuno, T.; Watanabe, T.; Suzuki, N.; Goto, T.; Yokoyama, K. Microstructure and silica mineralization of silicified woods I. Specimen identification of silicified woods and observations with a scanning electron microscope. *Mokozai Gakkaishi* **1986**, *32*, 387–400.
71. Furuno, T.; Watanabe, T.; Suzuki, N.; Goto, T.; Yokoyama, K. Microstructure and silica mineralization of silicified woods. II: Distribution of organic carbon and the formation of quartz in the structure of silicified woods. *Mokozai Gakkaishi* **1986**, *32*, 575–583.
72. Ballhaus, C.T.; Gee, K.; Greef, K.; Bockrath, C.; Mansfield, T.; Rhede, D. The silicification of trees in volcanic ash: An experimental study. *Geochim. Cosmochim. Acta* **2012**, *84*, 62–74.
73. Saminpanya, S.; Sutherland, F.L. Evidence of silica phase-transformations during diagenesis in petrified woods from Thailand area fluvial deposits. *Sediment. Geol.* **2013**, *290*, 15–26.
74. Augustithis, S.S. *Encyclopedia of Sphaeroidal Textures and Their Genetic Significance*; Theophrastus Publications: Athens, Greece, 1982; pp. 71–73, 241–250.

© 2015 by the authors; licensee MDPI, Basel, Switzerland. This article is an open access article distributed under the terms and conditions of the Creative Commons Attribution license (<http://creativecommons.org/licenses/by/4.0/>).